

# A MULTI-STAGE SHRINKING CORE MODEL FOR THERMAL DECOMPOSITION REACTIONS WITH A SELF-INHIBITING NATURE

Amirpiran Amiri <sup>1</sup>, Gordon D Ingram <sup>1</sup>, Andrey V Bekker <sup>2</sup>, Iztok Livk <sup>2</sup>, Nicoleta E Maynard <sup>1</sup>

<sup>1</sup>Department of Chemical Engineering, Curtin University  
GPO Box U1987, Perth, WA 6845, Australia  
[a.amiri@curtin.edu.au](mailto:a.amiri@curtin.edu.au)

<sup>2</sup>Parker Cooperative Research Centre for Integrated Hydrometallurgy Solutions,  
CSIRO Process Science and Engineering, Australia

## ABSTRACT

Among the variety of thermal decomposition reactions, some display self-inhibiting behaviour, where the produced gas negatively influences the reaction progress. Further, a build-up of internal pressure caused by the product gas may alter the reaction pathway over the reaction duration in a way that favours a particular pathway over others. Two well-known cases of this kind of reaction are the thermal decomposition of limestone and gibbsite, in which carbon dioxide and water vapour are the produced gases, respectively. A multi-stage, multi-reaction, shrinking core model is proposed for this type of reaction. The model emphasises the role of the produced gas, not only in the mass transfer rate, but also in the reaction kinetics. It also includes parallel and series reaction pathways, which allows for the presence of an intermediate species. The model has been applied to the conversion of gibbsite to alumina, and it includes the formation of boehmite as an intermediate product. The model results are in good agreement with experimental data for gibbsite calcination reported in the literature. Gibbsite conversion, boehmite formation and subsequent consumption, as well as alumina formation, are successfully simulated. Further, the corresponding kinetic parameters are estimated for all reactions of interest.

**Keywords:** multi-reaction model, self-inhibiting reaction, gibbsite calcination, alumina production, boehmite formation.

## INTRODUCTION

Many modelling efforts have been reported on both catalytic and non-catalytic gas-solid particle reactions using a variety of approaches depending upon the physical and chemical properties of the *solid* and the type of reaction considered. Comprehensive reviews of the major modelling categories and their features are given by Ramachandran & Doraiswamy (1982) and Molina & Mondragón (1998). The importance of developments in gas-solid reaction modelling is still high since a wide variety of reactions encountered in the process industries belong to this class. Combustion, gasification, roasting of sulphides, calcination, reduction of metal ores, and catalyst regeneration are typical industrial gas-solid processes demanding new modelling tools for process intensification and product design. Modelling becomes crucial when prediction and control of transients during reaction at high conversion rates and at high temperature is the subject of investigation. In such cases deeper insight will be achieved by carefully establishing the relationships between dominant mechanisms, including reaction kinetics and transport processes, as well as structural changes taking place over the reaction period. Further, the combination of different sub-models at different time and

length scales in a multi-scale modelling framework makes it possible to deal with product quality issues (small scale) via control of the process (large scale).

To date, particle reaction models have been mainly based on reactions with a positive order, particularly first order reactions. The variation of the reaction mechanism over the reaction period due to a change of internal conditions, like the build-up of gas pressure inside the particle, has not been extensively studied.

Mantri *et al.* (1976) proposed a three-zone model comprised of a core, an outer product layer and a reacting zone in between them. The model is based on a single reaction and it is assumed that the reaction is first order with respect to gas concentration and zero order with respect to the solid. This model was applied by Chang & Kuo (1999) to predict the transport of reactive gas in a packed bed of porous media. A variation of the shrinking core model with an intermediate layer was also proposed by Homma *et al.* (2005). In their work, fresh reactant is converted to an intermediate followed by conversion of the intermediate to a gas product without leaving any ash (solid) layer. This model was also based on a first order reaction with respect to the gaseous reactant. The intermediate component formed immediately and the final product was formed only via consumption of the intermediate. Suresh & Ghoroi (2009) developed a model for solid-solid reactions in series for a single particle. In their work, multiple reactions were considered and reaction rates were first order with respect to the solid concentrations.

The objective of this paper is to develop a new version of the shrinking core model for a particular class of gas-solid reactions in which the released gas reduces the reaction rate and changes the reaction mechanism, and in which an intermediate solid species may form. Calcination and thermal dehydration / decomposition of solid particles belong to this category of gas-solid reactions. The prediction of the formation and consumption of an intermediate species is a leading feature of this model. This kind of information is needed for maximization or minimization of the amount of the intermediate in the product via process control. The involvement of multiple reactions with different orders, and determination of a reaction-switching time are other notable features of this new version of the shrinking core model.

As a case study, the calcination of gibbsite to alumina, in which boehmite forms as an intermediate, is the focus of this article. Gibbsite calcination, which is an important stage in alumina production via the Bayer process, has been studied for many years. The majority of publications related to gibbsite calcination have focused on reaction kinetics and phase transitions (Stacey, 1987; Whittington & Ilievski, 2004; Wang *et al.*, 2006; Ruff *et al.*, 2008; Gan *et al.*, 2009; Zhu *et al.*, 2010). Little work has been reported on coupling hydrodynamics and reaction kinetics (Marsh, 2009), and no work appears to be available specifically on multi-scale modelling of alumina calcination equipment, apart from our own preliminary efforts (Amiri *et al.*, 2010). For gibbsite calcination, and similar thermal dehydration reactions, the gaseous species (water) is a reaction product, not a reactant, which is different from many other gas-solid reactions. There is a lack of particle-scale conversion and species distribution models for reactions of this type. This paper is part of a study to develop a multi-scale model for the thermal dehydration of gibbsite in a fluidised bed reactor. A single gibbsite particle undergoing calcination is studied in this paper to establish a predictive three-stage model for particle conversion at high temperatures relevant to industrial operations. The paper explores the effect of water vapour pressure inside the particle on competing reactions and it includes the reaction orders with respect to vapour concentration for the various gibbsite calcination reactions.

Parameter estimation is performed by using two sets of experimental data from Wang *et al.* (2006), then the model is validated against another data set at a different temperature. While gibbsite calcination is the focus of this paper, the model developed is general enough to be applied to other reactions in which a gaseous species is a reaction product only, for example pyrolysis of carbon-based materials, thermal decomposition of some organic and inorganic compounds, and the reduction of metal oxides.

## MODEL DEVELOPMENT

### Reaction kinetics and modelling assumptions

Unreacted core models for gas-solid reactions, in which the reaction rate is based on the reactant gas concentration, have been used in a wide range of applications in the literature. The majority of previous investigations have focused on gas-solid reactions that were generally represented by a reaction such as  $gas + solid \rightarrow solid + gas$ .

The reaction was usually assumed to have first order kinetics with respect to the reacting gas concentration. However, in several applications, including thermal dehydration, gas-phase species are reaction products only. In this study there is no gaseous reactant and three reactions are involved. The following stoichiometric equations are used to represent parallel and series gas-solid reactions in a single particle:



Species A is the solid reactant; B is the solid intermediate; D is the final solid product, which may be formed directly from A through reaction (1) or via B in reactions (2) and (3); and C is the gaseous product.

The assumptions on which the mathematical model stands are

- The particle is initially pure, non-porous species A.
- A reaction of the form of Eq. (1) initially takes place on the surface of the unreacted core to produce a gas and a porous product layer, which adheres to the solid core. After a particular reaction extent, the reactions of Eqs (2) and (3) begin, forming and consuming the layer of intermediate solid B. Details are given later.
- The gas species formed diffuses through the porous product and intermediate layers, and a pseudo-steady state gas-phase concentration profile exists in the two layers. The effective diffusion coefficient is assumed to be the same in both layers. The pseudo-steady state assumption is reasonably acceptable for gas-solid reactions as in the majority of cases the criterion  $C_{(g)} / C_{(s)} \leq 10^{-3}$  holds (Gómez-Barea & Ollero, 2006).
- The particle is spherical with constant outer diameter during the reaction.
- The mass transfer rate through the surrounding gas layer outside the particle is assumed to be very high, so that the gas concentration at the particle surface and in the bulk gas is the same.
- The particle temperature is spatially uniform, but may vary with time. The particle exchanges energy with its surroundings by a combined convection and radiation heat transfer coefficient.

Although competition between different reaction pathways can be assessed by comparing intrinsic reaction rate constants at the same conditions, more factors, however, need to be considered to evaluate the reaction pathway selectivity. For instance, heating rate, gas pressure inside the particle and particle size may alter the reaction mechanism to favour one pathway over others (Candela & Perlmutter, 1986). This issue will be discussed later. This study couples the reaction pathways given by Eqs (1)–(3) in a reacting particle model to investigate the effect of dominant parameters including reaction and diffusion rates.

Solid conversion is considered to be negatively affected by the presence of the gas product C. The reaction rate has been modelled as being proportional to the difference between the partial pressure of the gaseous reactant and the equilibrium partial pressure; however, we used the following expression with a flexible order for the surface reaction rate (Candela and Perlmutter, 1992):

$$(-r_s) = kC_{S0}C_C^n \quad (4)$$

where  $S = A$  or  $B$ ,  $n$  is negative, and the rate coefficient obeys the Arrhenius equation:

$$k = k_0 e^{(-E/RT)} \quad (5)$$

### Mathematical model description and development

In the model, the particle is converted over several stages as presented in Fig. 1. During the first stage ( $0 \leq t \leq t_{12}$ ), the reaction of A starts at the outer surface of the particle, forming porous solid D and gas C according to reaction (1). As the thickness of the D layer increases with the reaction progress, escape of the produced gas becomes more difficult due to internal diffusion resistance, causing higher gas pressure at the reaction front. At a certain level of C gas pressure, the reaction mechanism changes and intermediate species B begins to form via reaction (2), and this point marks the end of stage 1. In the first stage, therefore, the particle consists of an unreacted core of A surrounded by a layer of D.

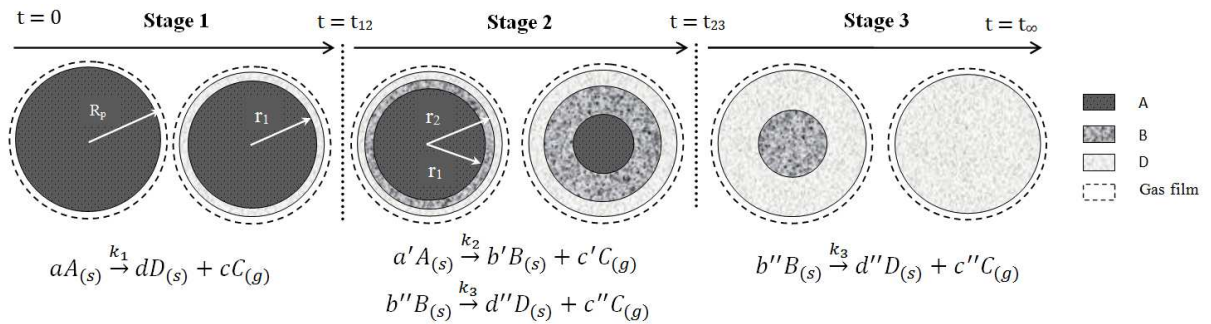


Fig. 1. Schematic of solid particle reaction including intermediate formation.

At time  $t_{12}$ , which marks the beginning of stage 2, the intermediate species B starts to form. The B then reacts to D via reaction (3). Thus, during stage 2, the particle has three zones – an inner unreacted core of A, a middle zone of the intermediate B, and an outer zone of product D. During stage 2, reactions (2) and (3) occur simultaneously at the A-B and B-D interfaces, respectively. Diffusive mass transfer of C also occurs in the intermediate and product layers.

The beginning of stage 3 occurs at time  $t_{23}$ , which happens when the A core disappears completely and the particle again has two zones – a B core and an outer product D layer. During this stage only reaction (3) is taking place at the B core surface. This stage ends with a completely converted particle that consists of D only.

Estimation of  $t_{12}$  and  $t_{23}$  is based on requiring continuity of the model predictions during the transition from stages 1 to 2, and stages 2 to 3, respectively. At  $t_{12}$ , the governing equations of stage 1 and stage 2 should predict the same radius and gas concentration at the core; in particular, Eqs (6) and (10) should both apply and yield  $r_1 = r_2 = r_{12}$  and  $C_{C1} = C_{C2} = C_{12}$  at  $t_{12}$ . Eqs (17) and (18), which are derived from Eqs (6) and (10), are therefore solved simultaneously for  $r_{12}$  and  $C_{12}$ , then  $t_{12}$  is deduced from Eq. (7) as the time taken for  $r_1$  to change from  $R_p$  to  $r_{12}$ . Calculation of  $t_{23}$  is more straightforward as it is the time when  $r_1 = 0$  according to Eq. (11).

The model equations for all three stages are summarized in Tab. 1.

Tab. 1: Governing equations of the three-stage shrinking core model.

<b>Stage 1</b>		
$C_{C1} - C_{Cs} - \frac{\vartheta_1 k_1 C_{C1}^{n_1} C_{A0}}{D_e} r_1^2 \left( \frac{1}{r_1} - \frac{1}{R_p} \right) = 0$		(6)
$-\frac{dr_1}{dt} = \frac{Mw_A}{\rho_A} k_1 C_{A0} C_{C1}^{n_1}$	$r_1 = R_p$ at $t = 0$	(7)
$\frac{R_p^3 \rho_e C_{pe}}{3Mw_e} \frac{dT}{dt} = R_p^2 h (T_b - T) - r_1^2 k_1 C_{A0} C_{C1}^{n_1} \Delta H_1$	$T = T_0$ at $t = 0$	(8)
<b>Stage 2</b>		
$C_{C1} - C_{C2} - \frac{\vartheta_2 k_2 C_{C1}^{n_2} C_{A0}}{D_e} r_1^2 \left( \frac{1}{r_1} - \frac{1}{r_2} \right) = 0$		(9)
$C_{C2} - C_{Cs} - \frac{\vartheta_2 k_2 C_{C1}^{n_2} C_{A0} r_1^2 + \vartheta_3 k_3 C_{C2}^{n_3} C_{B0} r_2^2}{D_e} \left( \frac{1}{r_1} - \frac{1}{R_p} \right) = 0$		(10)
$-\frac{dr_1}{dt} = \frac{Mw_A}{\rho_A} k_2 C_{A0} C_{C1}^{n_2}$	$r_1 = r_{12}$ at $t = t_{12}$	(11)
$-\frac{dr_2}{dt} = \frac{Mw_B}{\rho_B} k_3 C_{B0} C_{C2}^{n_3}$	$r_2 = r_{12}$ at $t = t_{12}$	(12)
$\frac{R_p^3 \rho_e C_{pe}}{3Mw_e} \frac{dT}{dt} = R_p^2 h (T_b - T) - r_1^2 k_2 C_{A0} C_{C1}^{n_2} \Delta H_2 - r_2^2 k_3 C_{B0} C_{C2}^{n_3} \Delta H_3$	$T = T_{12}$ at $t = t_{12}$	(13)
<b>Stage 3</b>		
$C_{C2} - C_{Cs} - \frac{\vartheta_3 k_3 C_{C2}^{n_3} C_{B0}}{D_e} r_2^2 \left( \frac{1}{r_2} - \frac{1}{R_p} \right) = 0$		(14)
$-\frac{dr_2}{dt} = \frac{Mw_B}{\rho_B} k_3 C_{B0} C_{C2}^{n_3}$	$r_2 = r_{23}$ at $t = t_{23}$	(15)
$\frac{R_p^3 \rho_e C_{pe}}{3Mw_e} \frac{dT}{dt} = R_p^2 h (T_b - T) - r_2^2 k_3 C_{B0} C_{C2}^{n_3} \Delta H_3$	$T = T_{23}$ at $t = t_{23}$	(16)
<b>Calculation of <math>r_{12}</math> and <math>C_{12}</math></b>		
$C_{12} - C_{Cs} - \frac{\vartheta_1 k_1 C_{12}^{n_1} C_{A0}}{D_e} r_{12}^2 \left( \frac{1}{r_{12}} - \frac{1}{R_p} \right) = 0$		(17)
$C_{12} - C_{Cs} - \frac{\vartheta_2 k_2 C_{12}^{n_2} C_{A0} r_{12}^2 + \vartheta_3 k_3 C_{12}^{n_3} C_{B0} r_{12}^2}{D_e} \left( \frac{1}{r_{12}} - \frac{1}{R_p} \right) = 0$		(18)

### Conversion and mass fractions

At any stage over the reaction period, the conversion of A and the mass fraction of each species in the particle can be calculated from the radius of the reaction front and the particle radius. The conversion of A is given by

$$1 - X(t) = \left( \frac{r_1}{R_p} \right)^3 \quad (19)$$

The mass fraction of a solid component in the particle can be calculated by

$$m_i(t) = \frac{n_i M w_i}{\sum_j n_j M w_j} \quad (20)$$

where  $M w_i$  and  $n_i$  are the molecular weight and number of moles of species  $i \in \{A, B, D\}$ .

### Model solution

The target variables to be determined at each stage are the core radii  $r_1$  and  $r_2$ , and the gas-phase C concentration  $C_C$ . The governing algebraic and differential equations were solved simultaneously along with the corresponding initial conditions to find the values of the target variables as functions of time.

### CASE STUDY

The calcination of gibbsite ( $\text{Al}(\text{OH})_3$ ) to alumina ( $\text{Al}_2\text{O}_3$ ) takes place mainly via two well-known reaction and phase transition pathways, one of which involves boehmite ( $\text{AlOOH}$ ). Heating rate, particle size distribution and water vapour pressure inside and around the particles are the main parameters that affect the reaction pathway. Regardless of any additional intermediate phases, the gibbsite calcination pathways may be summarized as:



A comparison of the gibbsite calcination reactions of Eqs (21)–(23) with the reactions of the general model, Eqs (1)–(3), indicates the following correspondence:  $A = \text{Al}(\text{OH})_3$ ,  $D = \text{Al}_2\text{O}_3$ ,  $B = \text{AlOOH}$ ,  $C = \text{H}_2\text{O}$ ,  $a = b'' = 2$ ,  $c = 3$ , and  $a' = b' = c' = c'' = d = d'' = 1$ .

According to Whittington & Ilievski (2004) and Candela & Perlmutter (1992), boehmite formation occurs more readily in the presence of high water vapour pressure and in large particles. However, even at high vapour pressures and for large particles (above 50  $\mu\text{m}$ ), the maximum boehmite mass fraction in a reacting gibbsite particle is reported as 30% by Whittington & Ilievski (2004).

In the above reactions, water vapour is a product and causes a barrier to reaction progress. The reaction rate equations include the influence of the water vapour concentration, and may include or exclude the solid concentration; for example, for the reaction of gibbsite, either of the following equations could apply:

$$-r_G = k_0 C_{G0} e^{(-E/RT)} C_A^n \quad (24)$$

$$-r_G = k_0' e^{(-E/RT)} C_G C_A^n \quad (25)$$

where  $n$  denotes the order of reaction and  $C_G$  and  $C_A$  represent the gibbsite concentration and water vapour concentration, respectively. In this study, the reaction rate was considered to be independent of the solid concentration, so Eq. (24) was used. Similar rate expressions were used for boehmite dehydration. The calcination of 75  $\mu\text{m}$  gibbsite particles at 473K and water vapour pressures in the range 100–3200 Pa was studied by Stacey (1987), who determined  $n$  values of  $-1.3$  and  $-0.4$  for gibbsite to alumina and boehmite to alumina conversions, respectively. Candela & Perlmutter (1986) estimated the value of  $n$  as  $-2$  for the reaction of gibbsite to alumina. Their investigation was done in a controlled, pure water vapour atmosphere at pressures from 50 to 3000 Pa over a temperature range from 458 to 508K.

### Parameter estimation and model validation

Wang *et al.* (2006) performed gibbsite calcination experiments at elevated temperature (823 to 923K) with a particle size range from 20 nm to 2000  $\mu\text{m}$ . Two of their data sets were used for parameter estimation and one for model validation. Most of the model's parameter values were taken from the literature as noted in Tab. 2. In our previous work (Amiri *et al.*, 2012), we focused on modelling the calcination of gibbsite to alumina via a 1-D distributed model that emphasised the role of vapour pressure and temperature dynamics inside the particle. Two of the key results obtained in the previous work were reasonable values for the reaction order with respect to water vapour concentration and the activation energy. In the current paper, four further parameters,  $k_{01}$ ,  $k_{02}$ ,  $k_{03}$  and  $E_3$ , were determined via least squares parameter estimation using the experimental data of Wang *et al.* (2006) at 898 and 923K according to

$$\min_{\substack{k_{01}, k_{02}, \\ k_{03}, E_3}} \sum_{S=A,B,D} \sum_{i=1}^N [m_{S,model}(i) - m_{S,expt}(i)]^2 \quad (26)$$

Fig. 2 demonstrates the good fit of the model to the data.

Tab. 2: Model parameters.

Parameter	Value	Reference / comment
$C_{pe}$ (J / mol.K)	80	Wefers & Misra (1987)
$D_e$ ( $\text{m}^2 / \text{s}$ )	$7 \times 10^{-10}$	Value for alumina; Fowler <i>et al.</i> (1977)
$R_p$ ( $\mu\text{m}$ )	50	Wang <i>et al.</i> (2006)
$E_1$ (kJ / mol)	131	Amiri <i>et al.</i> (2012)
$E_2$ (kJ / mol)	142	Ruff <i>et al.</i> (2008)
$E_3$ (kJ / mol)	145	Found by parameter estimation via Eq. (26)
$h(W / \text{m}^2.K)$	1.5	Incropera <i>et al.</i> (2007)
$k_{01}$ ( $\text{mol}^{-n} \text{m}^{3n+1} / \text{s}$ )	$6.18 \times 10^7$	Found by parameter estimation via Eq. (26)
$k_{02}$ ( $\text{mol}^{-n} \text{m}^{3n+1} / \text{s}$ )	$1.3 \times 10^6$	Found by parameter estimation via Eq. (26)
$k_{03}$ ( $\text{mol}^{-n} \text{m}^{3n+1} / \text{s}$ )	$3.5 \times 10^5$	Found by parameter estimation via Eq. (26)
$P_{Cb}$ (kPa)	3	Typical environmental water vapour pressure
$n_1$	-1	Amiri <i>et al.</i> (2012)
$n_2$	-0.5	Approximate value established in scoping studies
$n_3$	-0.4	Stacey (1987)
$T_b$ (K)	873–923	Experimental conditions of Wang <i>et al.</i> (2006)

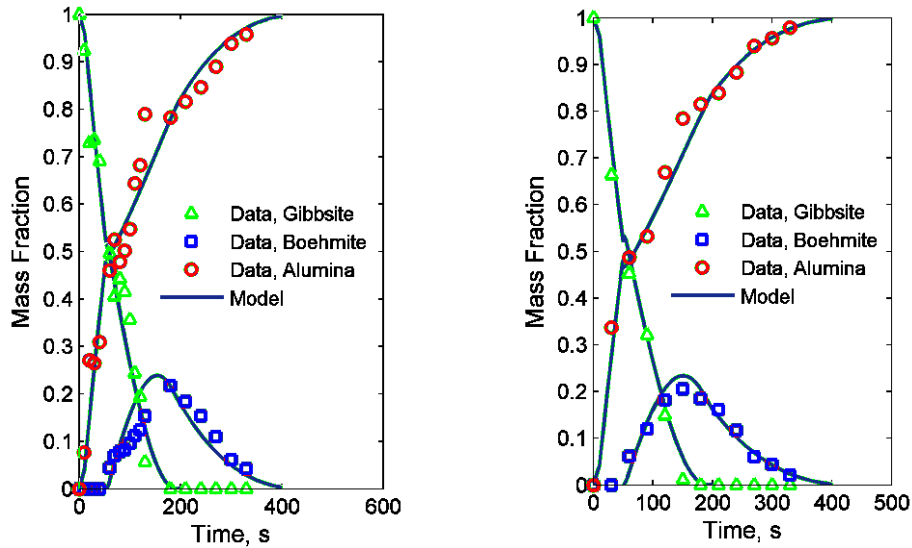


Fig. 2: Comparison of model predictions and experimental data (Wang *et al.*, 2006) at different environmental temperatures: 898K (left) and 923K (right).

### Comparison of single and multi-reaction scenarios

Fig. 3 compares the current model's predictions with those of a reduced version of the model in which boehmite formation is ignored and it is assumed that gibbsite reacts entirely according to Eq. (1). The full model reasonably predicts the depletion of gibbsite, the production and consumption of intermediate boehmite, and the production of alumina. The reduced model, however, offers a moderately acceptable prediction for gibbsite consumption, but overestimates the rate of alumina production and completely ignores the presence of boehmite. It should be noted that the same kinetic parameters are used in both full and reduced models in this comparison. While the single-stage model prediction for gibbsite consumption could be improved by a separate parameter fitting, it will still display unreasonable results for alumina and boehmite formation. Fig. 3 clearly shows the current multi-stage, multi-reaction model is superior to a single-stage, single-reaction model.

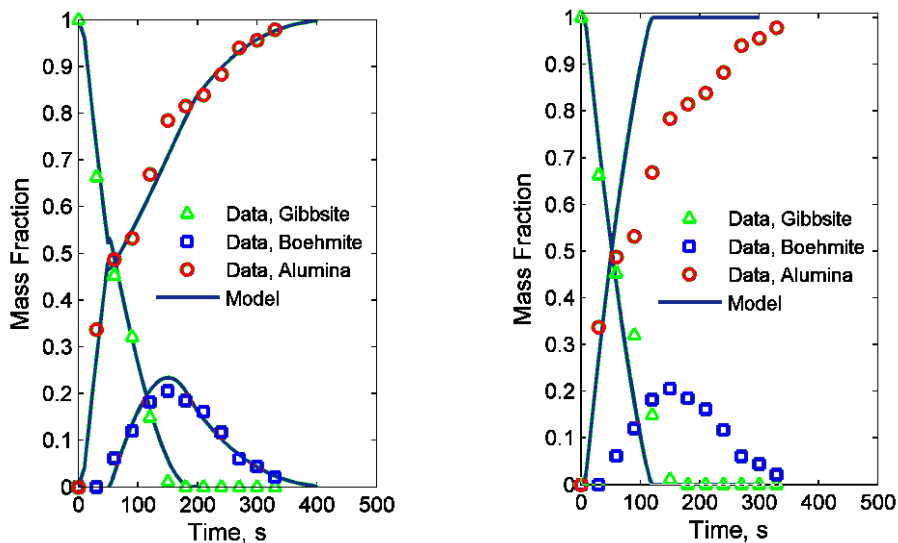


Fig. 3: Comparison of model predictions and experimental data (Wang *et al.*, 2006) at 923K: the multi-stage, multi-reaction model (left), and the reduced, single-reaction version (right).

## CONCLUSION

A multi-stage, multi-reaction, non-isothermal shrinking core model is proposed for gas-solid reactions with a self-inhibiting nature and in which a solid intermediate forms. The model consists of three stages and accounts for a transition in the reaction pathways. The proposed model displays good agreement with experimental data for the calcination of gibbsite to alumina with boehmite as an intermediate, and shows a significant improvement compared to a single-stage, single-reaction model.

## NOMENCLATURE

$a, c, d, a', b', c', b'', c'', d''$	Stoichiometric coefficients, [-]
$C_{A0}$	Initial fresh solid concentration, [mol/m <sup>3</sup> ]
$C_{B0}$	Initial intermediate solid concentration, [mol/m <sup>3</sup> ]
$C_{C1}$	Gas concentration at $r_1$ , [mol/m <sup>3</sup> ]
$C_{C2}$	Gas concentration at $r_2$ , [mol/m <sup>3</sup> ]
$C_{Cb}$	Gas concentration in surrounding environment, [mol/m <sup>3</sup> ]
$C_{Cs}$	Gas concentration on particle surface, [mol/m <sup>3</sup> ]
$C_{G0}$	Initial gibbsite concentration, [mol/m <sup>3</sup> ]
$C_{Pe}$	Effective heat capacity, [J/mol K]
$C_{12}$	Gas concentration at reactant-product interface at $t_{12}$ , [mol/m <sup>3</sup> ]
$D_e$	Effective diffusivity coefficient, [m <sup>2</sup> /s]
$D_p$	Particle diameter, [m]
$E$	Activation energy, [J/mol]
$\Delta H$	Heat of reaction, [J/mol]
$h$	Heat transfer coefficient, [W/m <sup>2</sup> K]
$k$	Surface reaction rate constant, [mol <sup>-n</sup> m <sup>3n+1</sup> /s]
$k_0$	Arrhenius pre-exponential coefficient, [mol <sup>-n</sup> m <sup>3n+1</sup> /s]
$M_w$	Molecular weight, [g/mol]
$M_{w_e}$	Average molecular weight, [g/mol]
$m$	Mass fraction, [-]
$n$	Reaction order with respect to water vapour concentration, [-]
$P_{Cb}$	Environmental gas (C) pressure, [kPa]
$R$	Gas constant, [J/mol K]
$R_p$	Particle radius, [m]
$r_G$	Gibbsite surface reaction rate, [mol/m <sup>2</sup> s]
$r_s$	Solid surface reaction rate, [mol/m <sup>2</sup> s]
$r_1$	Unreacted fresh reactant core radius at any time, [m]
$r_{12}$	Reactant-product interface location at $t_{12}$ , [m]
$r_2$	Intermediate-product interface location at any time, [m]
$r_{23}$	Intermediate-product interface location at $t_{23}$ , [m]
$T$	Temperature, [K]
$T_b$	Environmental temperature, [K]
$T_0$	Initial particle temperature, [K]
$T_{12}$	Particle temperature at $t_{12}$ , [K]
$T_{23}$	Particle temperature at $t_{23}$ , [K]
$t$	Time, [s]
$t_{12}$	Time for transition from stage 1 to 2, [s]
$t_{23}$	Time for transition from stage 2 to 3, [s]
$t_\infty$	Reaction completion time, [s]
$X$	Reactant conversion, [-]

### Greek symbols

$\vartheta_1, \vartheta_2, \vartheta_3$	Ratio of stoichiometric coefficients: $(c/a)$ , $(c'/a')$ , $(c''/b'')$ , [-]
$\rho_e$	Average density, [kg/m <sup>3</sup> ]

## REFERENCES

- Amiri, A, Bekker, A, Ingram, GD, Livk, I & Maynard, N 2012, 'A 1-D non-isothermal dynamic model for the thermal decomposition of a gibbsite particle', submitted to *Chemical Engineering Research and Design*.
- Amiri, A, Ingram, GD, Maynard, N, Livk, I & Bekker, A 2010, 'A multiscale modelling outlook for gibbsite calcination', in: *CD-ROM Proceedings of Chemeca 2010*, Adelaide, Australia, 26–29 September 2010.
- Candela, L & Perlmutter, DD 1986, 'Pore structure and kinetics of the thermal decomposition of  $\text{Al}(\text{OH})_3$ ', *AIChE Journal*, vol. 32, no. 9, pp. 1532–1545.
- Candela, L & Perlmutter, DD 1992, 'Kinetics of boehmite formation by thermal decomposition of gibbsite', *Industrial and Engineering Chemistry Research*, vol. 31, no. 3, pp. 694–700.
- Chang, Y-I & Kuo, J-A 1999, 'Application of the three-stage shrinking core model in the transport of reactive gas in the porous media', *Journal of Petroleum Science and Engineering*, vol. 22, no. 1–3, pp. 205–216.
- Fowler, JD, Chandra, D, Elleman, TS, Payne, AW & Verghese, K 1977, 'Tritium diffusion in  $\text{Al}_2\text{O}_3$  and BeO', *Journal of the American Ceramic Society*, vol. 60, no. 3–4, pp. 155–161.
- Gan, BK, Madsen, IC & Hockridge, JG 2009, 'In situ X-ray diffraction of the transformation of gibbsite to  $\alpha$ -alumina through calcination: Effect of particle size and heating rate', *Journal of Applied Crystallography*, vol. 42, no. 4, pp. 697–705.
- Gómez-Barea, A & Ollero, P 2006, 'An approximate method for solving gas-solid non-catalytic reactions', *Chemical Engineering Science*, vol. 61, no. 11, pp. 3725–3735.
- Homma, S, Ogata, S, Koga, J & Matsumoto, S 2005, 'Gas–solid reaction model for a shrinking spherical particle with unreacted shrinking core', *Chemical Engineering Science*, vol. 60, no. 18, pp. 4971–4980.
- Incropera, FP, DeWitt, DP, Bergman, TL & Lavine, AS 2007, *Fundamentals of Heat and Mass Transfer*, 6<sup>th</sup> edn, John Wiley, Hoboken.
- Mantri, VB, Gokarn, AN & Doraiswamy, LK 1976, 'Analysis of gas-solid reactions: Formulation of a general model', *Chemical Engineering Science*, vol. 31, no. 9, pp. 779–785.
- Marsh, C 2009, 'CFD Modelling of alumina calciner furnaces', in: *Seventh International Conference on CFD in the Minerals and Process Industries*, Melbourne, Australia, 9–11 December 2009.
- Molina, A & Mondragón, F 1998, 'Reactivity of coal gasification with steam and  $\text{CO}_2$ ', *Fuel*, vol. 77, no. 15, pp. 1831–1839.
- Ramachandran, PA & Doraiswamy, LK, 1982, 'Modeling of noncatalytic gas-solid reactions', *AIChE Journal*, vol. 28, no. 6, pp. 881–900.
- Ruff, TJ, Toghiani, RK, Smith, LT & Lindner, JS 2008, 'Studies on the gibbsite to boehmite transition', *Separation Science and Technology*, vol. 43, no. 9–10, pp. 2887–2899.
- Stacey, MH 1987, 'Kinetics of decomposition of gibbsite and boehmite and the characterization of the porous products', *Langmuir*, vol. 3, no. 5, pp. 681–686.
- Suresh, AK & Ghoroi, C 2009, 'Solid-solid reactions in series: A modeling and experimental study', *AIChE Journal*, vol. 55, no. 9, pp. 2399–2413.
- Wang, H, Xu, B, Smith, P, Davies, M, DeSilva, L & Wingate, C 2006, 'Kinetic modelling of gibbsite dehydration/amorphization in the temperature range 823–923 K', *Journal of Physics and Chemistry of Solids*, vol. 67, no. 12, pp. 2567–2582.
- Wefers, K & Misra, C 1987, 'Oxides and hydroxides of aluminium', *Technical Paper No. 19*, Alcoa Laboratories, Pittsburgh, PA.
- Whittington, B & Ilievski, D 2004, 'Determination of the gibbsite dehydration reaction pathway at conditions relevant to Bayer refineries', *Chemical Engineering Journal*, vol. 98, no. 1–2, pp. 89–97.
- Zhu, B, Fang, B & Li, X 2010, 'Dehydration reactions and kinetic parameters of gibbsite', *Ceramics International*, vol. 36, no. 8, pp. 2493–2498.